npj | digital medicine

Article

Published in partnership with Seoul National University Bundang Hospital

https://doi.org/10.1038/s41746-025-01625-y

# Digital twins enable stratification of persistent atrial fibrillation patients for ablation diminishing unnecessary heart damage



Kensuke Sakata[1], Carolyna A. P. Yamamoto[2], Adityo Prakosa[1], Brock M. Tice[1], Syed Yusuf Ali[2], Shane Loeffler[1], Eugene G. Kholmovski[1,2], Sunil Kumar Sinha[3], Joseph E. Marine[3], Hugh Calkins[3], David D. Spragg[3] & Natalia A. Trayanova[1,2] ✉

Pulmonary vein isolation (PVI), the standard-of-care for atrial fibrillation (AF), is effective even in some persistent AF (PsAF) patients despite atrial fibrosis proliferation, suggesting that PVI could not only be isolating triggers but diminishing arrhythmogenic substrates. Left atrial (LA) posterior wall isolation is the prevalent adjunctive strategy aiming to address PsAF arrhythmogenesis, however, its outcomes vary widely. To explore why current PsAF ablation treatments have limited success and under what circumstances each treatment is most effective, we utilized patient-specific heart digital twins of PsAF patients incorporating fibrosis distributions to virtually implement versions of PVI (individual ostial to wide antral) and posterior wall isolation. In most digital-twins (60%) PVI greatly decreased LA substrate arrhythmogenicity without the need of wider lesions or posterior wall isolation. Using digital-twin findings, a strategy was developed to stratify PsAF patients to an appropriate ablation option based on fibrosis features, thus potentially avoiding unnecessary heart damage.

Catheter ablation is an established therapy for rhythm control in atrial fibrillation (AF), the most common tachyarrhythmia[1,2]. Pulmonary vein (PV) isolation (PVI) to prevent electrical triggers in the PVs from spreading into the atria is the cornerstone ablation therapy for AF[3,4]. The persistent form of AF (PsAF) typically involves atrial fibrosis-remodeled substrates that can anchor or otherwise sustain reentrant wavefronts[5,6]. This paradigm suggests that PVI only—even when a durable wide circumferential antral isolation[7,8]—may be inadequate for the ablative treatment of PsAF. However, randomized trials have not shown favorable outcomes in PsAF beyond PVI alone[9–14]. These meta-analyses suggest that in some PsAF patients, likely those with fibrotic arrhythmogenic substrates, PVI may not only be isolating triggers but also diminishing the arrhythmogenic propensity of the atrial fibrotic substrate. However, the impact of PVI on the left atrial (LA) substrate has not been fully explored, and whether it depends on the specific PVI strategy[15–19] has not been addressed previously. Of the ablation strategies adjunctive to PVI, LA posterior wall isolation (PWI) is the one that has been explored most extensively, as it aims to address substrate arrhythmogenicity in PsAF. However, results vary considerably across different studies[20–22], and the causes of this large variation are not known. Understanding the impact of PVI and PWI strategies on the patient-specific arrhythmogenic substrates in PsAF and for which patients each of these treatments would be most appropriate could have a major impact on AF ablation efficacy, AF management, the associated healthcare expenditures, and patient well-being.

Digital twinning is an emerging technology that utilizes cardiac imaging and electrophysiological data to generate multi-scale (from the cell to the organ) personalized computational models of the electrical functioning of a patient's heart[23]. Digital twins (DTs) of patient's atria reconstructed from late gadolinium-enhancement cardiac MRI (LGE-MRI), which visualizes fibrosis, have been used for non-invasive testing of the arrhythmogenic propensity of the atrial fibrotic substrate[24]; have demonstrated, in a pilot prospective study[25], the ability to directly guide the delivery of lesions that reduce the likelihood of AF occurrence in PsAF patients; and have been used to develop an extra-PVI ablation strategy that could minimize lesions[26] while also decreasing the potential for iatrogenic tachycardia[27]. The mechanistic underpinning of the DT technology also allows for the

[1]Alliance for Cardiovascular Diagnostic and Treatment Innovation, Johns Hopkins University, Baltimore, MD, USA. [2]Department of Biomedical Engineering, Johns Hopkins University, Baltimore, MD, USA. [3]Division of Cardiology, Department of Medicine, Johns Hopkins University School of Medicine, Baltimore, MD, USA. ✉e-mail: ntrayanova@jhu.edu

exploration of the advantages and limitations of different strategies for ablation currently in existence as well as their relation to the patient-specific atrial substrates underlying PsAF.

Here, we utilize atrial DT technology in a prospective observational clinical study to investigate the arrhythmogenic properties of the atrial fibrotic substrate in patients with PsAF and determine the circumstances under which PVI strategies and PWI ablation are effective in diminishing the LA substrate arrhythmogenic propensity. We elucidate the fibrotic remodeling substrate features of the PsAF patients' atria that render them benefitting from the different ablation strategies without causing unwarranted damage to atrial tissue. Our results provide new clarity in the understanding of the effect of standard-of-care ablation strategies on the arrhythmogenic substrate and provide a novel approach to patient selection for a specific AF ablation approach. The results of this study are expected to lead to effective strategies in mitigating patients' AF burden while sparing healthy tissue from destruction and to a decrease in ablation redo procedures. Based on digital-twin findings, a strategy was developed to stratify PsAF patients to an appropriate ablation option based on features of their atrial fibrosis distribution.

## Results

### Patients characteristics

From the 48 participants undergoing MRI examination, thirteen patients were excluded from this study: nine with poor quality of images, three with no evidence of atrial fibrosis, and one having a variant anatomy with large persistent left superior vena cava. Personalized DTs of the remaining 35 patients were created and used in the analyses of fibrosis distribution and potential substrate arrhythmogenicity, characterized by substrate locations capable of sustaining persistent reentrant activations (locations of reentry, LRs) (Fig. 1, **top row**); these patients and their DTs characteristics are presented in Table 1. The average age was 66 years. A large proportion of participants was male (77%), and the majority of them had a BMI > 30 (60%). Twelve patients had a history of prior PVI procedure without any substrate modification outside PVI. Except for two patients not having ablation procedural data: one canceled the ablation procedure and the other had no data stored owing to a hardware malfunction, electro-anatomical mapping data were analyzed in 33 patients (Fig. 1, **bottom row**).

### LRs identified in the DTs

For all 35 DTs, the total number of all LRs characterizing the different DT arrhythmogenic substrates was 195. Among all 195 LRs, 108 LRs were in LA (i.e., LA-LR) and 87 in the right atrium (RA), as shown in Fig. 2a; the LRs in the RA were unaffected by any of the ablation strategies. It is notable that among the 108 LRs in the LA, 63 LRs (58%) were found inside the wide antral PVI (WA-PVI) lesions. The majority of them were at the posterior side of the PVI lesions in DTs (35 LRs, 56%). These results suggest that WA-PVI plays an important role in substrate modification. Indeed, the regions encircled by WA-PVI lesions had significantly higher values of fibrosis fraction (FF, see Methods) and proportion of locations with high fibrosis entropy (FE, see Methods) than the LA regions outside WA-PVI lesions; 19% [12–29] vs. 15% [11–18] for FF ($p = 0.002$); 57 ± 16% vs. 49 ± 12% for proportion of locations with high FE ($p = 0.003$) (Supplementary fig. 1). This indicates that the regions encircled by WA-PVI had high propensity to arrhythmogenesis.

### Efficacy of each ablation strategy in decreasing LA substrate arrhythmogenic propensity

Out of 108 LA-LRs in the entire DT cohort, PWI + PVI eliminated 74 LA-LRs (69%), while WA-PVI eliminated 65 (60%, with 63 LA-LRs enclosed by WA-PVI lines, and two eliminated by WA-PVI itself as described below) ($p = 0.016$ for PWI + PVI vs. WA-PVI; McNemar's test). The individual ostial PVI (IO-PVI) eliminated 53 LA-LRs (49%) ($p = 0.001$ for WA-PVI vs. IO-PVI; McNemar's test) (Fig. 2b). Remarkably, in two DTs, a total of two LRs, located at the LA posterior wall and at the LA roof, disappeared after WA-PVI because reentry dynamics at these locations was affected by the nearby lesion, and the reentry could not be sustained. Similarly, in four DTs, a total of six LRs disappeared outside the PWI + PVI lesions after adding PWI to WA-PVI. Of these, four LRs in four DTs, each located at the LA

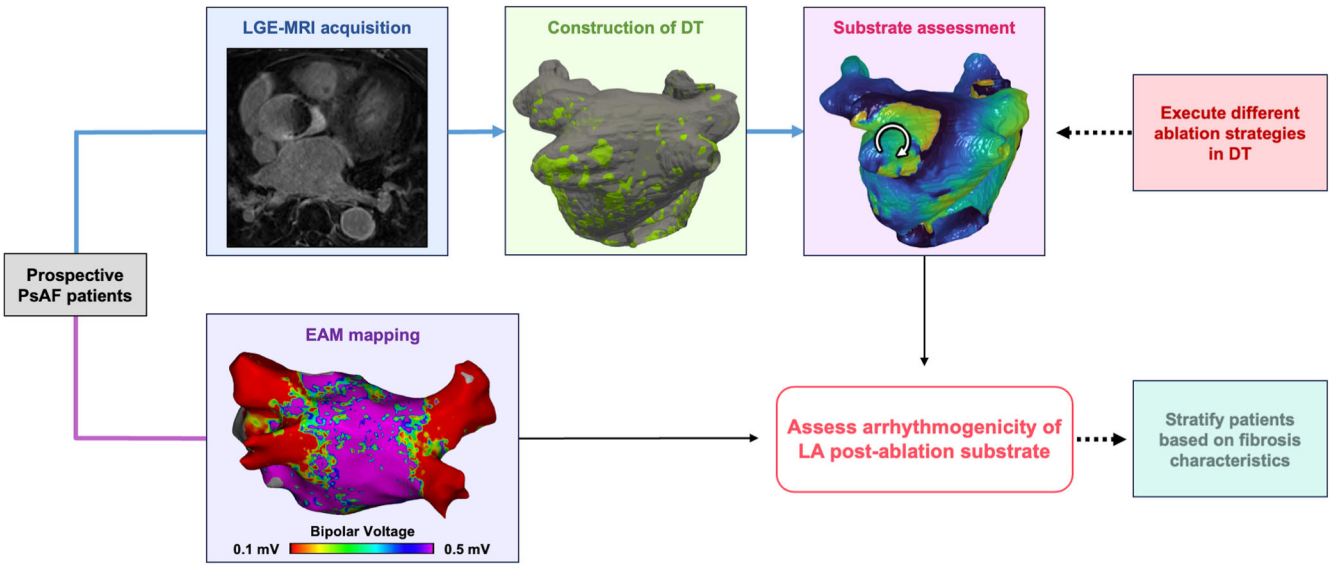


**Fig. 1 | Overview of this study.** Consecutive PsAF patients were prospectively enrolled in this study. LGE-MRI images were acquired prior to the ablation procedure (light-blue panel), which served as the basis for the generation of personalized bi-atrial DTs that incorporated the patient-specific fibrosis distribution (light-green panel). Following the substrate inducibility test, LRs were identified (reentrant activation shown with arrow in light-magenta panel). Next, IO-PVI, WA-PVI and PWI + PVI ablation strategies were executed virtually in each DT, and their efficacy on diminishing the arrhythmogenic propensity of the LA substrate was quantified. During each ablation procedure (bottom row), EAM data in sinus rhythm was acquired to investigate the presence of LVA (light-purple panel) and examine whether LVAs can be predictors of the benefit of the PWI + PVI strategy. Finally, these features of fibrotic substrate were utilized to stratify patients benefitting from each ablation strategy. DT digital twin, EAM electro-anatomical map, IO-PVI individual ostial PVI, LA left atrial, LGE-MRI late gadolinium enhancement-magnetic resonance imaging, LR location of reentry, LVA low-voltage area, PsAF persistent atrial fibrillation, PVI pulmonary vein isolation, PWI + PVI left atrial posterior wall isolation plus WA-PVI, WA-PVI wide antral PVI.

https://doi.org/10.1038/s41746-025-01625-y



**Table 1 | Characteristics of patients and their DTs**

| | Entire DT cohort (N = 35) | DTs with added benefit of PWI over WA-PVI (*N* = 8) | DTs where added PWI was not beneficial (*N* = 27) | *P* value | DTs where WA-PVI was more beneficial than IO-PVI (*N* = 6) | DTs where WA-PVI was not more beneficial than IO-PVI (*N* = 21) | *P* value |
|---|---|---|---|---|---|---|---|
| **Clinical information** | | | | | | | |
| **Male** | 27 (77) | 5 (63) | 22 (82) | 0.346 | 6 (100) | 16 (76) | 0.555 |
| **Age, Y** | 66 [59–73] | 72 [63–76] | 63 [58–70] | 0.169 | 62 [47–68] | 63 [59–71] | 0.335 |
| **Body Mass Index, kg/m$^2$** | 30.6 ± 4.6 | 29.3 ± 3.4 | 31.0 ± 4.9 | 0.355 | 31.8 ± 5.8 | 30.8 ± 4.8 | 0.692 |
| **$CHA_2DS_2$-VASc score** | 2 [1–3] | 3 [1–4] | 2 [1–3] | 0.412 | 2 [0–3] | 2 [1–3] | 0.655 |
| **Left ventricular ejection fraction, %** | 54.7 ± 8.7 | 56.9 ± 11.5 | 54.1 ± 7.8 | 0.437 | 54.5 ± 11.1 | 54.0 ± 7.0 | 0.893 |
| **History of previous PVI** | 12 (34) | 1 (13) | 11 (41) | 0.216 | 4 (67) | 7 (33) | 0.187 |
| **Days from MRI to ablation, days** | 19 [14–23] | ·· | ·· | ·· | ·· | ·· | ·· |
| **Global LA information** | | | | | | | |
| **LA volume, ml** | 132 [113–173] | 116 [102–135] | 140 [117–176] | 0.132 | 138 [122–145] | 140 [115–181] | 0.977 |
| **FF in the LA, %** | 16 ± 6 | 19 ± 6 | 15 ± 6 | 0.091 | 21 ± 7 | 13 ± 5 | 0.004* |
| **The number of LA-LRs** | 3 [2–4] | 5 [3–5] | 3 [2–4] | 0.019* | 4 [3,4] | 2 [2,3] | 0.018* |
| **Local substrate features** | | | | | | | |
| **LAPW volume, cm$^3$** | 2.94 ± 0.85 | 2.78 ± 0.83 | 2.99 ± 0.86 | 0.551 | ·· | ·· | ·· |
| **FF within LAPW, %** | 9 [6–16] | 21 [10–28] | 8 [4–13] | 0.009* | ·· | ·· | ·· |
| **Proportion of high FE locations within LAPW, %** | 50 ± 23 | 66 ± 13 | 45 ± 24 | 0.028* | ·· | ·· | ·· |
| **≥ 10% LVA at LAPW** | 4 (12) | 1 (13) | 3 (12) | 1.000 | ·· | ·· | ·· |
| **PV antrums volume, cm$^3$** | 2.66 ± 1.19 | ·· | ·· | ·· | 2.66 ± 1.92 | 2.71 ± 1.08 | 0.935 |
| **FF within PV antrums, %** | 20 [11–26] | ·· | ·· | ·· | 28 [18–50] | 17 [10–21] | 0.157 |
| **Proportion of high FE locations within PV antrums, %** | 51 ± 16 | ·· | ·· | ·· | 51 ± 19 | 48 ± 15 | 0.659 |

Values are the mean ± S.D., the median [Q1-Q3] or *n* (%).

*$p < 0.05$, statistically significant.

*DT* digital twin, *FE* fibrosis entropy, *FF* fibrosis fraction, *IO-PVI* individual ostial PVI, *LA* left atrial, *LAPW* LA posterior wall, *PWI + PVI* LAPW isolation plus WA-PVI, *LVA* low-voltage area, *LRs* locations of reentry, *MRI* magnetic resonance imaging, *PV* pulmonary vein, *PVI* PV isolation, *WA-PVI* wide antral PVI.

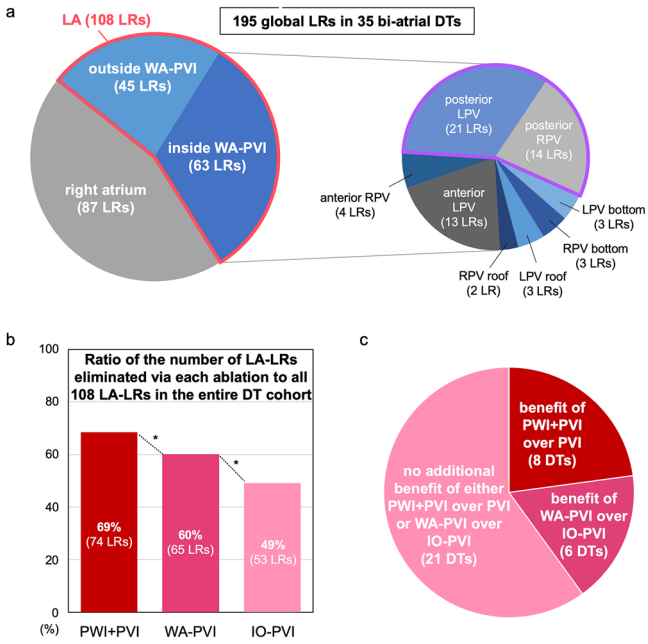


**Fig. 2 | LA-LR distribution and the efficacy of each ablation strategy.** **a** Distribution of LRs identified in all bi-atrial DTs. **b** Comparison of the ratio of the number of LA-LRs eliminated via each ablation strategy to all LA-LRs in our DT cohort. **c** DTs classification based on the efficacy of each strategy in LA substrate improvement. DT digital twin, IO-PVI individual ostial PVI, LA left atrium, LPV left PV, LR location of reentry, PV pulmonary vein, PVI PV isolation, PWI + PVI LA posterior wall isolation plus WA-PVI, RPV right PV, WA-PVI wide antral PVI. *$p < 0.05$.

posterolateral wall, at the LA inferior wall, at the LA lateral, and at the LAA-PV ridge, disappeared because reentry dynamics there was affected by the nearby lesion. Finally, in two DTs, two LRs at the LA inferoposterior wall disappeared because parts of the meandering trajectories of the reentries overlapped with the bottom line of PWI. These findings indicate that some of the ablation strategies executed in the patient's DTs influenced the arrhythmogenic propensity of the substrate and affected the LRs outside of the ablation lesions.

However, among the DTs of the 35 patients in this study, 27 (77%) did not benefit from the additional PWI lines in terms of improving the DTs substrate propensity to arrhythmia, as measured by the LA-LR number (Fig. 2c). Furthermore, among the latter 27 DTs, in 21 DTs (78%), there was no additional benefit of WA-PVI over IO-PVI, and PWI lines also made no difference (Fig. 2c). In six DTs that benefitted from WA-PVI over IO-PVI, four had previous PVI lesions and two had no prior PVI history, however, the number of LRs inside WA-PVI areas was comparable among them (3 [2,3] vs. 2 [2,3], $p = 0.803$). These DT results indicate that, while extensive ablation lesions could contribute significantly to the decrease in LA substrate arrhythmogenicity, most of the cases examined did not require such extensive lesions.

Figure 3 presents two typical cases. In the first example, the number of LA-LRs was five; their trajectories of phase singularity of the reentry were shown in Supplementary Fig. 2a. LR 1, located at the bottom of the right inferior PV, LR 2 at the posterior carina of the right PV, and LR 3 at the LA posterior wall were eliminated by PWI + PVI (60% improvement of the LA substrate). In contrast, WA-PVI in the same DT was able to eliminate LR 1 and LR 2, but not LR 3 (40% improvement). Consequently, this case demonstrated that PWI + PVI was more effective than WA-PVI in decreasing LA substrate arrhythmogenic propensity (Fig. 3a). In the second example, the number of LA-LRs characterizing the LA substrates was three: LR 1 at the anterior antrum of the right PV, LR 2 at the posterior carina of the right PV, and LR 3 at the posterior carina of the left PV; their trajectories of phase singularity of the reentry were shown in Supplementary Fig. 2b. Executing PWI + PVI or WA-PVI eliminated all three LRs (100% LA substrate improvement). However, IO-PVI was unable to eliminate LR 3 (67% benefit). Therefore, in this case, while PWI + PVI was not more effective than WA-PVI, the latter was more effective than IO-PVI in decreasing the arrhythmogenic propensity of the LA substrate (Fig. 3b). Additionally, Supplementary Fig. 3 presents two more typical cases. As shown in Supplementary fig. 4, in only one case across the entire DT cohort, both PVI and PWI were unable to eliminate any LRs despite the fact that there were only two LRs in the LA; one was at the upper lateral LA, and the other was at the inferolateral LA.

## Relationship between features of the LA fibrotic substrate and the benefit of adding PWI to WA-PVI

The differences between the DTs in which there was benefit of executing PWI lines and those in which there was not, are presented in Table 1. Values of FF in the LAs in the DTs that demonstrated benefit of adding PWI to WA-PVI were higher than those in the DTs that did not have that benefit, with borderline significance (LA FF: 19 ± 6% vs. 15 ± 6%, $p = 0.091$) (Fig. 4a). Additionally, the number of LRs in the LAs was also significantly greater in these DTs (LA-LR number: 5 [3–5] vs. 3 [2–4], $p = 0.019$). The volumes of the LA posterior walls were comparable between these two groups of DTs (2.78 ± 0.83 $cm^3$ vs. 2.99 ± 0.86 $cm^3$, $p = 0.551$), however both FF and the proportion of locations with high FE at the LA posterior walls in the DTs demonstrating benefit of the added PWI were significantly higher than those in the other group of DTs; 21% [10–28] vs. 8% [4–13] for FF within LA posterior wall ($p = 0.009$) (Fig. 4b); 66% ± 13% vs. 45% ± 24% for proportion of locations with high FE values within the LA posterior wall ($p = 0.028$) (Fig. 4c). These fibrotic substrate features are illustrated in the example presented in Fig. 3a.

In contrast, inferring from the intra-procedure electrograms, among the 33 DTs (excluding two DTs that did not have electro-anatomical mapping data), there was no significant difference in the presence of low-voltage areas (LVAs) at the LA posterior wall between the two groups of DTs (13% vs. 12%, $p = 1.000$) (Fig. 4d). For predicting whether there is a benefit of adding PWI to PVI, the cut-off values were FF in the LA of 19% with an AUC of 0.690 (0.477–0.902) (74% accuracy), FF within the LA posterior wall of 9% with an AUC of 0.801 (0.644–0.958) (69% accuracy) and proportion of locations having high FE within the LA posterior wall of 50% with an AUC of 0.764 (0.603–0.925) (66% accuracy) (Fig. 4e). Based on these DT results, it is reasonable to assume that as long as our methodology is applied, when patients' LA posterior walls have FF > 9% or the proportion of high FE

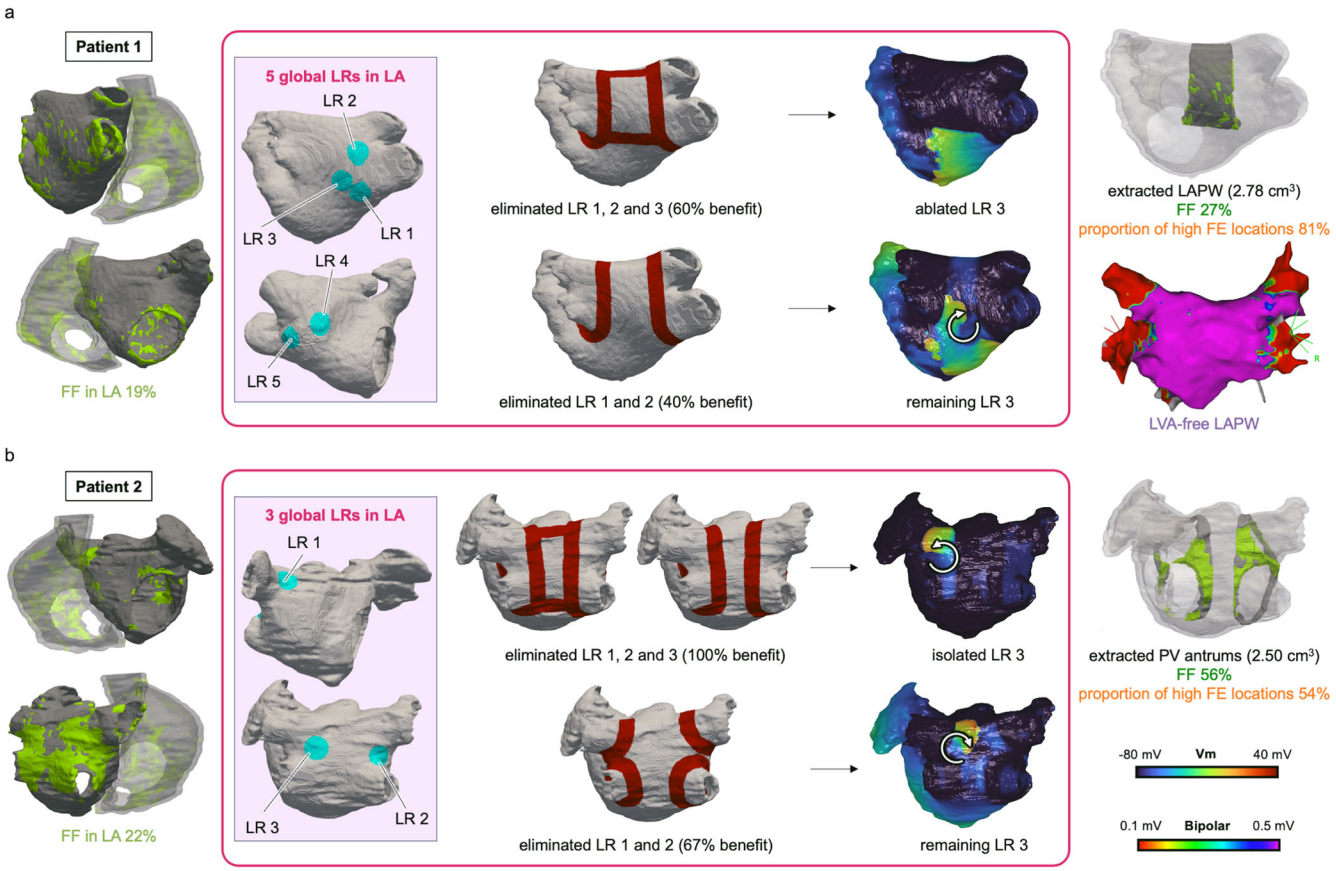


**Fig. 3 | Examples of differential efficacy of each strategy. a** A patient for whom there was an added benefit of PWI over WA-PVI in decreasing LA arrhythmogenesis in the DT. The patient's DT incorporating fibrosis (light-green), with LA-LR distribution (light-blue dots), virtual ablation (red lines) representing PWI + PVI (top) and WA-PVI (bottom) lesions, probing post-ablation inducibility and identifying the eliminated and remaining LRs (white circular arrows indicating reentry), and investigation of the features of the fibrosis (top) and the electro-anatomical map (bottom) at LAPW. **b** A patient for whom added PWI was not beneficial over WA-PVI, but WA-PVI provided added benefit over IO-PVI in eliminating LA-LRs. The patient's DT incorporating fibrosis (light-green), with LA-LR distribution (light-blue dots), virtual ablation (red lines) representing PWI + PVI (top-left), WA-PVI (top-right), and IO-PVI (bottom) lesions, probing post-ablation inducibility and identifying the eliminated and remaining LRs (white circular arrows indicating reentry), and investigation of the features of the fibrosis at PV antrums. DT digital twin, FE fibrosis entropy, FF fibrosis fraction, IO-PVI individual ostial PVI, LA left atrium, LAPW LA posterior wall, LR location of reentry, LVA low-voltage area, PVI pulmonary vein isolation, PWI + PVI LAPW isolation plus WA-PVI, WA-PVI wide antral PVI.

locations occupies > 50% of that wall, it would be beneficial to consider PWI to achieve LA substrate improvement. Otherwise, the addition of PWI to PVI may only lead to unnecessary ablation.

### Relationship between features of the LA fibrotic substrate and the benefit of WA-PVI ablation instead of IO-PVI

The differences between the DTs where WA-PVI was more beneficial than IO-PVI in reducing arrhythmogenic propensity of the LA substrate and those where it was not are also shown in Table 1. The LAs in the DT group that demonstrated benefit of WA-PVI over IO-PVI had significantly greater FF than that in the DT group that did not demonstrate that benefit (21 ± 7% vs. 13 ± 5%, $p = 0.004$) (Fig. 4f). In addition, the number of LA-LRs was also significantly greater in these DTs (LA-LR number: 4 [3,4] vs. 2 [2,3], $p = 0.018$). For predicting whether WA-PVI ablation will be more beneficial than IO-PVI, the cut-off value of FF in the LA was 14% with an AUC of 0.857 (0.701–1) (70% accuracy) (Fig. 4g). In the PV antrums, both FF and proportion of locations with high FE were higher in the DTs demonstrating benefit of WA-PVI over IO-PVI than in those that did not, although there was no statistical significance; 28% [18–50] vs. 17% [10–21] for FF within PV antrums ($p = 0.157$) (Fig. 4h); 51% ± 19% vs. 48% ± 15% for proportion of high FE locations within PV antrums ($p = 0.659$) (Fig. 4i). These fibrotic substrate features are illustrated in the example presented in Fig. 3b. The volumes of the PV antrums did not exhibit significant difference between the two groups of DTs (2.66 ± 1.92 $cm^3$ vs. 2.71 ± 1.08 $cm^3$, $p = 0.935$). This might imply that, provided that our DT methodology is used, when FF is over 14% in the LA, while in the LA posterior wall FF is ≤ 9% and the proportion of locations in that wall with high FE is ≤ 50%, wider PVI line configurations could provide additional benefit lesions in diminishing the arrhythmogenic propensity of the LA substrate. Otherwise, extensive PVI lesions spreading widely into the LA body are not more beneficial than the minimal ostial PVI. Figure 5 summarizes these findings in a patient stratification flowchart.

## Discussion

Our goal in this prospective observational-clinical and personalized digital-twinning study was to elucidate the roles of both the standard treatment, PVI, and the prevalent adjunctive strategy, PWI, in decreasing the arrhythmogenic propensity of PsAF patients' LA substrates, and to uncover LA substrate features that can be used to best stratify patients for these strategies. We found that WA-PVI—designed for trigger isolation[3,4,7,8]—eliminated 60% of all LA-LRs in the DT cohort, decreasing the arrhythmogenic potential of LA substrates. This finding might explain why PVI succeeds in many PsAF patients and why ad-hoc strategies for targeting the extra-PVI substrates have had limited success. We found that PWI eliminated more LA-LRs than WA-PVI (69% vs. 60%) in the DT cohort, and WA-PVI was also significantly more beneficial than IO-PVI (60% vs. 49%) in diminishing LA substrate arrhythmogenicity. However, 77% of all DTs had no benefit from PWI; in these DTs, execution of the additional PWI

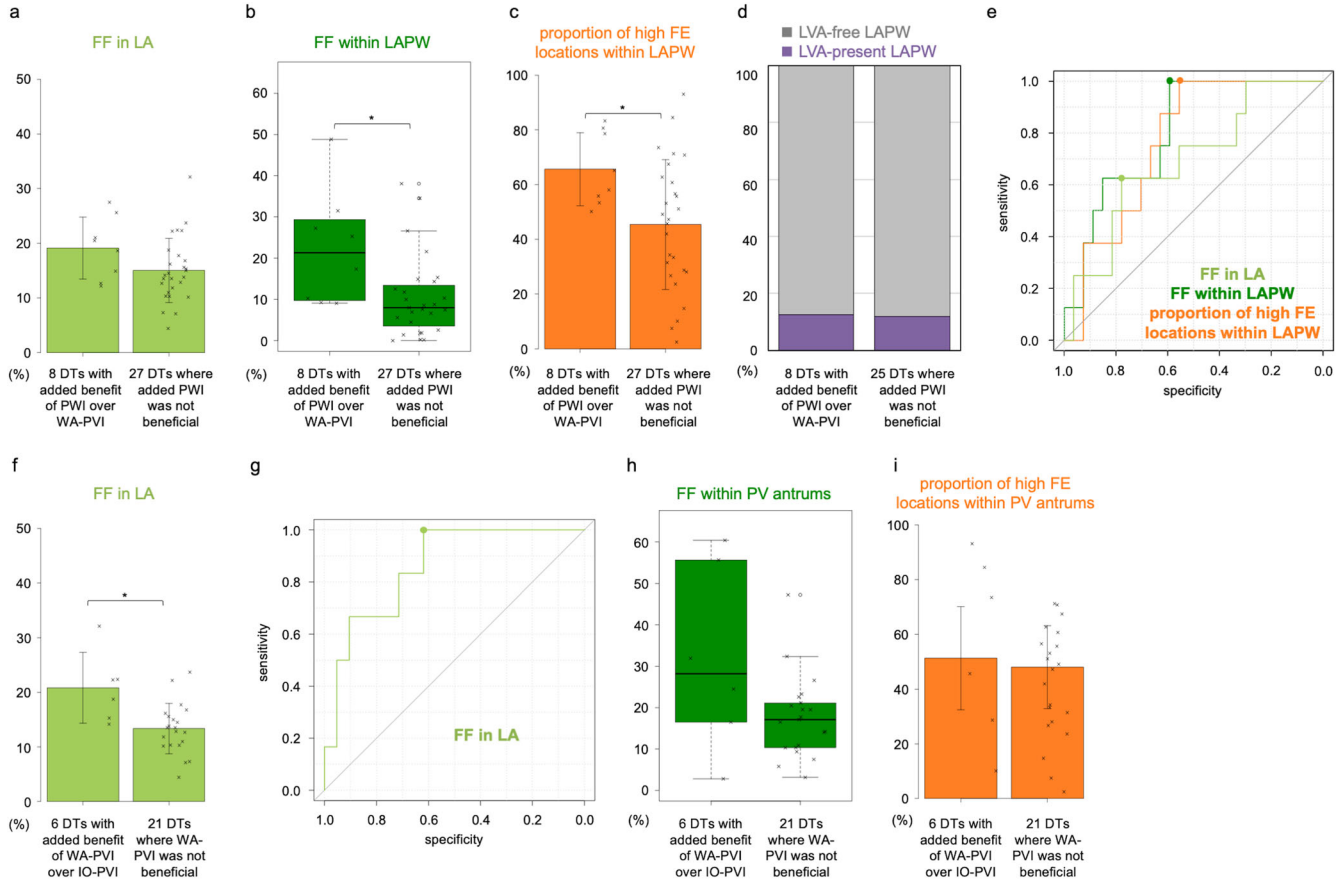


**Fig. 4 | Relationships between ablation strategies and substrate features.** **a** Comparison of FF in the LA between DTs with added benefit of PWI over WA-PVI and those without. **b** Comparison of FF within LAPW between DTs with added benefit of PWI over WA-PVI and those without. **c** Comparison of proportion of high FE locations within LAPW between DTs with added benefit of PWI over WA-PVI and those without. **d** Comparison of LVA at LAPW between DTs with added benefit of PWI over WA-PVI and those without. **e** Receiver operating characteristic curve for predicting the benefit of PWI when added to WA-PVI. **f** Comparison of FF in the LA between DTs with added benefit of WA-PVI over IO-PVI and those without. **g** Receiver operating characteristic curve for predicting the benefit of WA-PVI over IO-PVI ablation. **h** Comparison of FF within PV antrums between DTs with added benefit of WA-PVI over IO-PVI and those without. **i** Comparison of proportion of high FE locations within PV antrums between DTs with added benefit of WA-PVI over IO-PVI and those without. DT digital twin, FE fibrosis entropy, FF fibrosis fraction, IO-PVI individual ostial PVI, LA left atrium, LAPW LA posterior wall, LVA low-voltage area, PV pulmonary vein, PVI PV isolation, PWI + PVI LAPW isolation plus WA-PVI, WA-PVI wide antral PVI. *$p < 0.05$. Circle and cross marks represent outliers and data points, respectively.

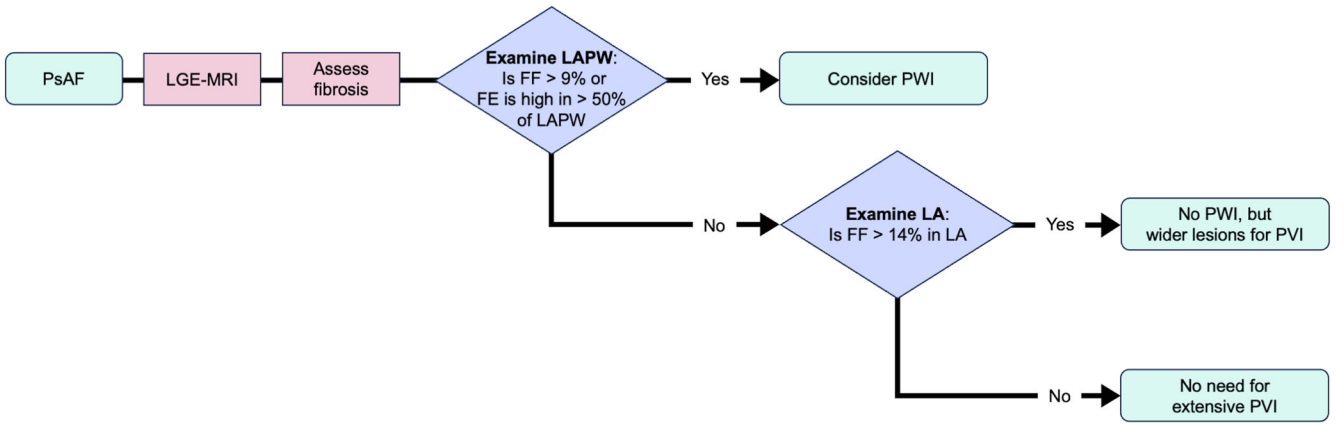


**Fig. 5 | Flowchart to stratify patients benefitting from each ablation strategy.** Fibrosis assessment could be useful for properly stratifying patients benefitting from PWI or wider PVI. FE fibrosis entropy, FF fibrosis fraction, LA left atrium, LAPW LA posterior wall, LGE-MRI late gadolinium enhancement-magnetic resonance imaging, PsAF persistent atrial fibrillation, PVI pulmonary vein isolation, PWI LAPW isolation.

lines would have resulted in large unnecessary ablations. Furthermore, among these DTs, 78% had no benefit of WA-PVI over IO-PVI. Importantly, we identified that in the DTs, FF > 9% and the proportion of locations having high FE > 50% within the LA posterior wall were indicators for improvement with PWI (AUC 0.801 and 0.764). FF in the LA > 14% were found to predict the benefit of wider configurations of PVI lines (AUC 0.857). In contrast, the presence of LVA at the LA posterior wall was not a predictor of the potential benefit of PWI over PVI. These findings might suggest that evaluating LGE-MRI scans can help determine which patients will benefit from PWI or wider PVI, as we propose in the flowchart in Fig. 5.

Over the last two decades, various approaches to detection and ablation of AF substrates have been proposed for PsAF treatment. However, clinical trial investigators have reported that the variety of approaches to LA substrate ablation (extra-PVI ablation) have provided no consistent clinical benefit over PVI alone[9–14]. While it could be expected that PVI, an across-the-board approach, would have variable efficacy for patients with individual substrates, it is noteworthy that its efficacy has been comparable to that of any ad-hoc or even patient-specific extra-PVI strategies, such as intra-atrial electrograms-guided ablation[28–32]. This observation suggests that PVI plays a crucial role not only in trigger elimination but in LA substrate improvement, a role that our present study elucidated. Our study also uncovered that over half of the LA-LRs eliminated by standard WA-PVI in our DT cohort were located at the posterior sides of PVI lines where delivery of different ablation energy to prevent esophageal injury is required. This finding highlights the fact that PVI efficacy in eliminating LA substrate arrhythmogenicity could be affected by lesion configurations and durability in these areas based on the operators' discretion[33].

Our results demonstrate that out of all LA-LRs in our DT cohort, PWI, a common adjunctive strategy to PVI, eliminated significantly more LA-LRs than standard PVI alone. This finding is consistent with a recent study reporting that linear ablations including PWI was the most effective extra-PVI strategy for PsAF substrate ablation despite the possibility that iatrogenic atrial tachyarrhythmias due to conduction gaps along ablation lines could negate its benefit[34]. To address incomplete ablation lesions and corresponding gaps, new approaches and technologies such as high-power short-duration ablation and pulse field ablation are aiming to improve durability of lesions[15,35] and thus, the outcomes of PWI[21]. On the other hand, our finding that over three-quarters of the individual PsAF patient DTs did not benefit from PWI also aligns with findings from recent clinical trials reporting inconsistent outcomes of PWI[20–22]. These results suggest that even if durable PWI can be achieved, it would be desirable to appropriately select the patients for its application to avoid unnecessary ablation and injury to the atria. Indeed, a number of reports have highlighted the fact that extensive substrate ablation carries a high risk of gaps and scar-related reentry and the corresponding post-ablation iatrogenic atrial tachycardia[32,34,36], and it also can cause stiff LA syndrome, impairing atrial diastolic function[37].

Current clinical PVI lesions typically lie between the lines of WA-PVI and IO-PVI chosen here. Our study demonstrated that among all LA-LRs in our DT cohort, larger numbers of LA-LRs were eliminated as the lesions were moved from IO-PVI to WA-PVI. This explains why different clinical PVI lesions executed with different tools and approaches[4,7,8,15–19] result in a wide range of efficacies in LA substrate modification. However, over three-quarters of PsAF patients' DTs did not benefit from WA-PVI over IO-PVI, explaining the results of recent reports that cryoablation, which creates wider lesions compared to radiofrequency ablation[38], worsened atrial function[39] and was not superior to radiofrequency in rhythm control[16]. This suggests that not all patients require wider PVI lines, highlighting the importance of appropriately selecting patients who are likely to benefit from more extensive lesion configurations. Impact on atrial tissue is often downplayed in the intensive pursuit of durable PVI. Indeed, recent studies have demonstrated that PVI lesions via cryo-, hot- and laser-balloon, pulse field ablation, and high-power short-duration radiofrequency[17,38,40] or those guided by a higher lesion-quality marker[41] were all significantly larger than those via conventional catheter radiofrequency. Thus, efficacy being equal in diminishing LA substrate arrhythmogenicity, it is desirable to select an ablation strategy that minimizes lesions. Finally, it should be acknowledged that the PV antrums and the LA posterior wall could harbor triggers involved in AF persistence[42]; indeed, the posterior wall has been reported to be a frequent site of non-PV foci[43]. Thus, while the majority of PsAF patients' DTs here did not benefit from PWI or wider PVI in terms of improving the arrhythmogenic substrate, these ablation strategies might contribute to trigger isolation in these patients.

In this study, we used the personalized DTs to determine the features of the LA fibrotic substrate that can be used to assign PsAF patients to a particular ablation strategy. In patients with FF > 9% or proportion of high FE locations > 50% within the LA posterior wall, a typical region of fibrosis remodeling[44], PWI + PVI was found, with good predictive performance (AUC 0.801 and 0.764, respectively), to be beneficial in diminishing LA arrhythmogenic propensity. Interestingly, we also found that presence of LVA in the LA posterior wall was not predictive of PWI benefit in LA substrate improvement. We also investigated another low-voltage cut-off value, this time 1.08 mV for unipolar voltage[45], however, the results did not change. While LVA has been reported to be associated with clinical outcomes in recent studies[46–48], our finding is consistent with results from a recent study showing that additional PWI in patients with LVA in the LA posterior wall did not improve AF recurrence compared to PVI alone[47]. Our results also indicate that endocardial LVA, detected by bipolar mapping and standard cut-off voltages, which has been shown to be a predictor of AF and cardiac disease, is not an appropriate ablation target. Our DT results demonstrate that among patients that would not benefit from PWI, those with FF in the LA > 14% would be candidates for WA-PVI with high prediction performance (AUC 0.857). In the absence of these features, wider antral lesions may not be needed for PVI. Throughout this study, we have emphasized the importance of an optimal approach to patient selection for PsAF ablation. While wider ablation lesions would provide a higher probability of diminishing substrate arrhythmogenicity, more extensive ablation leads to increase in the likelihood of negative impacts on the healthy atrium. If patients are properly stratified, utilizing our DT technology or other potential biomarkers, then the damage currently inflicted indiscriminately in the atria could be decreased.

Finally, our study focused on the ablation strategies that are designed to suppress arrhythmogenesis in the LA. However, as our results demonstrate, there is a significant number of LRs in the RAs of the patients in this cohort. The RA has been typically overlooked in clinical research[44,49,50] and clinical trials[11,12,14,28–30,32]. However, our results, here and in previous publications[25,26], indicate that there is often significant fibrosis in the RA; this is consistent with a number of published results. Developing effective strategies to mitigate the RA fibrosis-induced arrhythmogenesis and thus increase the efficacy of AF ablation would be an important advancement in AF management.

This study has several limitations. First, the population of the prospective study is small. However, in total over 100 ablation strategies and 4,000 substrate induction tests were virtually performed in the DTs of 35 consecutive patients. Next, the PVI and PWI lesions in the DTs mimic the lines drawn in the clinical ablation procedure in the same way as configurations of PVI lesions are designed using 3D images reconstructed from computed tomography scans or 3D EAM maps before ablation application[22], however, these lines vary, naturally, by practitioner and this cannot be fully captured in the DT. Finally, the present study utilized a digital-twinning approach to elucidate why PVI and PWI strategies have a wide range of outcomes in PsAF and to determine the features of the fibrotic substrate that can be used to stratify patients, and consequently, its conclusions need to be validated in clinical studies.

In conclusion, the present study, a combination of a prospective observational study and a digital-twinning technology, elucidated the roles of both PVI and PWI in reducing LA substrate arrhythmogenicity in patients with PsAF. PVI had a considerable effect in eliminating LA-LRs. Furthermore, most PsAF patients' DTs did not benefit from additional PWI. Fibrosis presence in the LA and its features can be used to stratify patients to an appropriate ablation option, potentially avoiding unwarranted heart

damage. Our DT technology incorporating fibrosis information could be useful for personalizing strategies for PsAF ablation pre-procedure.

## Methods

### Study design

In this prospective observational study, 48 PsAF patients scheduled for PsAF ablation at the Johns Hopkins Hospital were enrolled consecutively. The study was approved by the institutional review board of Johns Hopkins University (study number IRB00183327), and informed consent was obtained from all participants. The patients had no prior history of LA substrate ablation. Patients for whom the fibrotic distribution could not be assessed by LGE-MRI due to the inability to maintain sinus rhythm during MRI, or who had low fibrosis burden of <5% (indicating lack of arrhythmogenic substrate) were excluded. LGE-MRI images were acquired prior to ablation and were used in creating DTs of the patients' fibrotic atria. Electro-anatomical maps were obtained during the ablation procedure. The personalized DTs were used in simulation of different ablation strategies investigating their effectiveness in eliminating the arrhythmogenic substrate of each patient, and, in combination with electro-anatomical mapping analysis, in exploration of substrate features that influenced ablation efficacy. Simulations and the analysis of their data were conducted blinded to the electro-anatomical mapping. Figure 1 presents an overview of this study.

### Cardiac MR acquisition

Cardiac MRI scans were acquired for constructing patient-specific DTs before the catheter ablation procedure using a 1.5 Tesla MRI system (Aera; Siemens Healthineers, Erlangen, Germany) (Fig. 1, **blue-framed image**). MRI study protocol and technical characteristics have been previously described in detail[24–27]. Briefly, the protocol included contrast-enhanced MR angiography to visualize the atria and PV anatomy, and LGE-MRI scans to assess atrial fibrosis. Patients were given antiarrhythmic drugs to maintain stable sinus rhythm needed for high-resolution three-dimensional LGE-MRI acquisition; pre-MRI electrical cardioversion was administered as needed. Contrast-enhanced MR angiography was acquired using TWIST (Siemens Healthineers, Erlangen, Germany) pulse sequence in coronal orientation with a gadolinium contrast agent (gadobutrol; Bayer Healthcare Pharmaceuticals, Montville, NJ). LGE-MRI were acquired in axial orientation using electrocardiogram-gating and respiratory navigator 20–25 minutes after contrast administration.

### Personalized digital twinning

The methodology for creating patient-specific bi-atrial DTs has been described in detail in our previous publications[24–27], with its utility in ascertaining the patient's atrial arrhythmogenic substrate demonstrated in prospective studies[25,26]. Briefly, three-dimensional fibrosis distributions were reconstructed by semi-automatic segmentation of LGE-MRI scans (Fig. 6a) using the deep neural network CLARAnet[51]. Quality control was performed using the image-processing software ITK-SNAP (http://www.itksnap.org). To discern fibrotic tissue, a new personalized image intensity ratio method, described in our recent publications[26,27], was used, where the intensity threshold for atrial fibrosis was based on the mean value of atrial blood pool and reference fibrous tissue for each patient to minimize effects of multiple factors (including contrast dose, delay time, heart rate, and contrast clearance) on image intensity ratio between atrial wall and blood pool. Moreover, this personalized method showed high reproducibility of fibrosis distribution between the two images of a given pair of LGE-MRI scans acquired during the same imaging session[26,51]. In this study, enhancement in the LGE-MRI comprised both non-ablation native fibrosis and prior ablation scar since the latter becomes indistinguishable from the former over time. Once the personalized fibrosis distribution was generated (Fig. 1, **green-framed image**), voxels segmented from the LGE-MRI scans were transformed into a three-dimensional tetrahedral mesh using the commercial 3D medical modeling software Materialise Mimics (Materialise HQ, Leuven, Belgium), with a target edge length of 300 μm. Fiber orientations reconstructed from diffusion tensor MRI data[52] were projected onto these meshes using a customized three-dimensional mapping software[53]. The comprehensive methodology and parameters for electrophysiological properties in the fibrotic substrate of PsAF patients' DTs were detailed in a number of previous publications[24–27]. Finally, all computational simulations were conducted on a parallel computing system using the freely available software openCARP (https://opencarp.org/)[54].

### Identification of arrhythmogenic substrates in the DTs

Once the personalized atrial DTs were reconstructed, we assessed the arrhythmogenic propensity of the fibrotic substrate in each DT. This was done by determining LRs (Fig. 1, **pink-framed image**). Each of those, if formed following the pacing train described below, would drive fibrillatory activity in the atrial DT, however, it is important to highlight that LRs are not necessarily representative of the specific AF episode dynamics in the patient, as they capture the arrhythmogenic propensity of the fibrotic substrate. As in our previous works[24–27], presence of LRs was probed by an inducibility test, consisting of the delivery of incremental burst pacing sequentially at 40 bi-atrial sites, the latter designed to represent locations of potential triggers (Fig. 6b). Once a sustained reentry was induced at a location in the substrate, defined as lasting for over 5 s, we recorded the trajectory of phase singularities of that reentry using the open-source visualization software Meshalyzer (https://github.com/cardiosolv/meshalyzer) and denoted the center of that trajectory area as LR (Fig. 6c). A bi-atrial fibrotic distribution could give rise to a few LRs, with the reentry at each LR being inducible from one or more pacing sites.

The number of *unique* LRs that can form in each bi-atrial DT substrate characterizes the arrhythmogenic potential of that fibrotic substrate. In this study, we use only the LA portion of this number (i.e., LA-LR) to characterize the LA substrate arrhythmia propensity in each DT, as all the examined standard ablation strategies described below target the LA only.

### Executing virtual PVI lesions in the personalized DTs

To investigate the impact of PVI lesions on LA PsAF substrates, in this study we designed two different configurations of PVI lesions—IO-PVI[3,4] and WA-PVI[7,8]—since the current clinical PVI lesions delivered via various ablation tools would fall between these PVI lines, i.e., outside IO-PVI but inside WA-PVI (Fig. 6d and e). Linear ablation lesions for both PVI strategies were created in each DT and applied in their entirety at once to the native fibrotic substrate, wherein myocardial tissues, i.e., normal and/or fibrotic tissues, were replaced with non-conductive scar at lesion locations, as described in our previous studies[24–27]. After each virtual IO-PVI or WA-PVI, we assessed the arrhythmogenic propensity of the new LA post-ablation substrate (native fibrosis + PVI lesions) in each DT by repeating the inducibility test from the same pacing locations and identifying the number of LRs in the LA. Then, to analyze how the ablation lines had affected the LRs that existed in the native substrate, for each DT, we determined the ratio of the number of LRs eliminated (ablated or isolated) in the LA by each PVI strategy to the original number of LA-LRs for this DT, as described in the preceding section. We used this ratio to qualitatively characterize the efficacy of each PVI strategy (the "benefit").

### Adding PWI to WA-PVI in the personalized DTs

Next, we applied PWI to each post-WA-PVI DT to explore the effect of this adjunctive strategy on the DT substrate. PWI entailed adding two linear lesions to WA-PVI; one line between the roof of the left superior PV and that of the right superior PV, and another line between the bottom of the left inferior PV and that of the right inferior PV (Fig. 6f)[20,22]. The inducibility test was then repeated post-PWI + PVI and the propensity to arrhythmia in the LA was again quantified in terms of LR presence. We similarly determined the benefit for this ablation strategy by calculating the ratio of the number of LRs eliminated or isolated in the LA via PWI + PVI in each DT to the original number of LA-LRs.

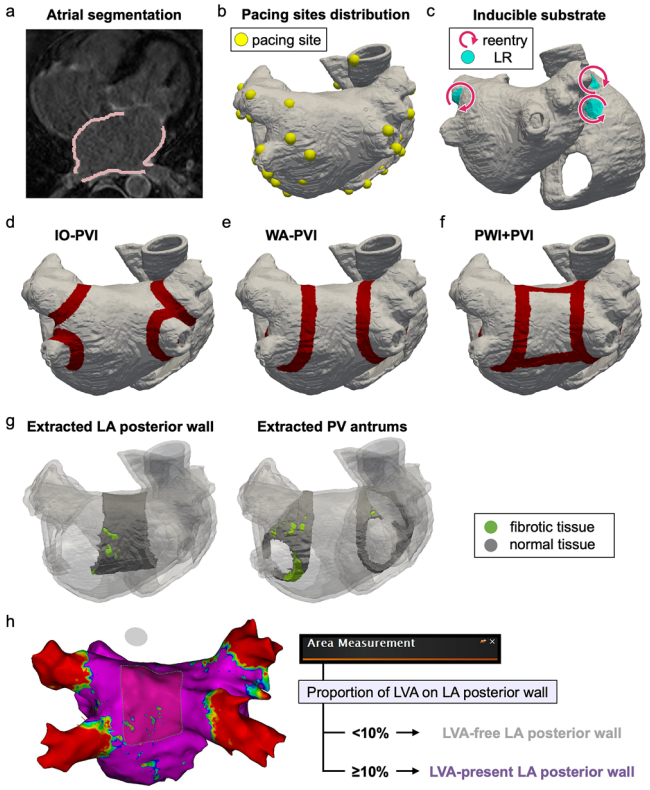


**Fig. 6 | Illustration of the methodologies in the study. a** Segmentation of the atrial wall (pink area). **b** Induction of reentry by burst pacing at 40 bi-atrial sites (yellow points). **c** LRs, locations of reentry (light blue areas); the rotational wavefront at each LR is indicated by the pink circular allow. **d** Configuration of the IO-PVI lesions. **e** Configuration of the WA-PVI lesions. **f** Configuration of the PWI + PVI lesions. **g** (left) LA posterior wall extracted between the WA-PVI lesions and the two PWI additional lesions. (right) PV antrums extracted between the WA-PVI and IO-PVI lesions. **h** Evaluation of LVA presence at the LA posterior wall using the CARTO area measurement tool. IO-PVI individual ostial PVI, LA left atrial, LR location of reentry, LVA low-voltage area, PV pulmonary vein, PVI PV isolation, PWI + PVI LA posterior wall isolation plus WA-PVI, WA-PVI wide antral PVI.

### Comparing ablation strategies in terms of their efficacy in modifying the LA arrhythmogenic substrate

In each DT, we compared the efficacy of each ablation strategy in decreasing arrhythmogenicity of the LA substrate. Specifically, we first examined the benefit of PWI + PVI over WA-PVI in improving the LA substrate (i.e., in decreasing the number of LA-LRs). Next, we determined whether WA-PVI was more effective in decreasing the number of LA-LRs than IO-PVI.

### Features of the LA fibrotic substrate, as derived from LGE-MRI, in DTs where ablation strategies diminished the arrhythmogenic propensity of the substrate

Similar to our previous publications[24,26,27], we used measures of how prevalent fibrosis is in a given region of the LA (the entire LA, LA posterior wall, and PV antrums) and what is the local level of interdigitation of fibrotic and non-fibrotic tissue in that region (i.e., the local level of fibrosis spatial disorganization, or FE) to characterize the LA fibrotic substrate. Specifically, we defined the ratio of the volume of the fibrotic tissue to that of the total tissue within a specific region, the FF, which was calculated using the freely available software ParaView (https://www.paraview.org). Next, three-dimensional maps of FE in the LA were constructed based on the local FE value at a given location in the LA calculated using the FE values at surrounding elements within a 2.5-mm radius, a kernel size equal to the resolution of LGE-MRI. Higher local values of FE signify areas of higher level of spatial disorganization in the fibrosis distribution, typically fibrosis border zones, previously shown to strongly promote arrhythmogenesis[24]. Therefore, we explored how prevalent such locations were in a given atrial region by determining all locations within the region with local FE values higher than the median local FE values of the same regions for all DTs. The measure of spatial disorganization of fibrosis in a given atrial region was then defined as the proportion of locations (points in the DT) with high FE out of all points in that region.

In each DT where PWI + PVI was more effective than WA-PVI in decreasing arrhythmogenicity of the LA substrate, the LA posterior wall (LA atrial wall outside WA-PVI lines but inside PWI + PVI lines) was extracted from the LGE-MRI images (Fig. 6g, **left**) and the FF value and proportion of locations having high FE within the LA posterior wall were analyzed.

Similarly, in DTs where WA-PVI was more effective than IO-PV in diminishing the arrhythmogenic substrate, PV antrums were extracted from the images (the areas outside the IO-PVI lines but inside the WA-PVI lines, Fig. 6g, **right**), and FF and proportion of locations having high FE within the PV antrums were calculated.

### Features of the LA fibrotic substrate, as derived from intra-atrial electrograms, in DTs where PWI + PVI was more effective than WA-PVI in diminishing the arrhythmogenic propensity of the substrate

For all patients, we analyzed the LA electro-anatomical maps (Fig. 1, **purple-framed image**) to determine the presence of LVAs. LVAs have been conventionally utilized as an indicator of arrhythmogenic substrate. The intra-atrial electrograms were acquired during the ablation procedure by trans-septal approach to the LA via the sheaths from femoral veins. Using a multi-electrode mapping catheter (PentaRay or OctaRay, Biosense Webster, Inc., CA) and an electro-anatomical map system (CARTO-3, Biosense Webster, Inc., CA), low voltage during sinus rhythm or stable pacing at the coronary sinus was defined as bipolar amplitude of <0.5 mV[28,29,46,47]. The patients' DTs were categorized into those with LVA in the LA posterior wall and those without, based on whether the proportion of LVA on the LA posterior wall surface was 10% or more (Fig. 6h)[29,30]. In the case of LVAs being present, their surface areas were determined manually using the area measurement tool in CARTO.

### Statistics analysis

Numerical variables were represented as the mean ± SD and the median [Q1–Q3] for normally and non-normally distributed data, respectively. Normal distribution was evaluated using a histogram and/or the combination with Shapiro-Wilk normality test and quantile-comparison plot. Depending on distribution, tests for statistical significance were performed using two-sided t-tests or Mann-Whitney U tests. Categorical variables were represented as the n (%) and compared using Fisher's exact tests. To compare the efficacy of each ablation strategy in modifying substrates, McNemar's Chi-squared test was used. Sensitivity, specificity, and accuracy were calculated using the ROC curves and the AUC to determine the cutoff for factors. The confidence interval of the AUC was estimated based on DeLong's test. The optimal cut-off value for prediction was determined using Youden's index, which maximizes the sum of sensitivity and specificity. A $p < 0.05$ was considered statistically significant for all tests.

All statistical analyses were conducted with EZR software, which is a graphical user interface for R (The R Foundation for Statistical Computing, Vienna, Austria); we used a modified version 1.55 of R commander designed to add statistical functions frequently used in biostatistics.

## Data availability

The anonymized datasets used and/or analyzed during the current study are available from the corresponding author on reasonable request. Raw scan image data and clinical electroanatomic mapping data cannot be shared for patient privacy reasons. Specific requests for access to these data may be made in consultation with the Johns Hopkins Institutional Review Board.

## Code availability

The image-processing software ITK-SNAP (v4.0.0) is freely available from http://www.itksnap.org. Computational meshes were generated using the commercial 3-matic (v15.0) analysis software (Materialise Mimics, Materialise HQ, Leuven, Belgium). All simulations were performed using the freely available openCARP software (v8.2) from https://opencarp.org. Simulation results were visualized using the freely available software Meshalyzer (v5.2) from https://github.com/cardiosolv/meshalyzer and analyzed using the open-source Visualization Toolkit-based software ParaView (v5.11) from https://www.paraview.org. Intra-atrial electrogram data were analyzed using the commercial EAM system (CARTO-3, Biosense Webster). All statistical analyses were conducted with EZR software (v1.55). The EZR data and codes will be made available upon request by contacting the corresponding author.

Received: 21 November 2024; Accepted: 9 April 2025;
Published online: 07 May 2025

## References

1. Friberg, L., Tabrizi, F. & Englund, A. Catheter ablation for atrial fibrillation is associated with lower incidence of stroke and death: data from Swedish health registries. *Eur. Heart J.* **37**, 2478–2487 (2016).
2. Camm, A. J. et al. The increasing role of rhythm control in patients with atrial fibrillation: JACC State-of-the-Art Review. *J. Am. Coll. Cardiol.* **79**, 1932–1948 (2022).
3. Haïssaguerre, M. et al. Electrophysiological end point for catheter ablation of atrial fibrillation initiated from multiple pulmonary venous foci. *Circulation* **101**, 1409–1417 (2000).
4. Pappone, C. et al. Circumferential radiofrequency ablation of pulmonary vein ostia: A new anatomic approach for curing atrial fibrillation. *Circulation* **102**, 2619–2628 (2000).
5. Platonov, P. G., Mitrofanova, L. B., Orshanskaya, V. & Ho, S. Y. Structural abnormalities in atrial walls are associated with presence and persistency of atrial fibrillation but not with age. *J. Am. Coll. Cardiol.* **58**, 2225–2232 (2011).
6. McDowell, K. S. et al. Mechanistic inquiry into the role of tissue remodeling in fibrotic lesions in human atrial fibrillation. *Biophys. J.* **104**, 2764–2773 (2013).
7. Oral, H. et al. Catheter ablation for paroxysmal atrial fibrillation: segmental pulmonary vein ostial ablation versus left atrial ablation. *Circulation* **108**, 2355–2360 (2003).
8. Benali, K. et al. Recurrences of atrial fibrillation despite durable pulmonary vein isolation: The PARTY-PVI Study. *Circ. Arrhythm. Electrophysiol.* **16**, e011354 (2023).
9. Verma, A. et al. Approaches to catheter ablation for persistent atrial fibrillation. *N. Engl. J. Med.* **372**, 1812–1822 (2015).
10. Vogler, J. et al. Pulmonary vein isolation versus defragmentation: The CHASE-AF clinical trial. *J. Am. Coll. Cardiol.* **66**, 2743–2752 (2015).
11. Inoue, K. et al. Pulmonary vein isolation alone vs. more extensive ablation with defragmentation and linear ablation of persistent atrial fibrillation: the EARNEST-PVI trial. *Europace* **23**, 565–574 (2021).
12. Marrouche, N. F. et al. Effect of MRI-Guided Fibrosis Ablation vs Conventional Catheter Ablation on Atrial Arrhythmia Recurrence in Patients With Persistent Atrial Fibrillation: The DECAAF II Randomized Clinical Trial. *JAMA* **327**, 2296–2305 (2022).
13. Spitzer, S. G. et al. Randomized evaluation of redo ablation procedures of atrial fibrillation with focal impulse and rotor modulation-guided procedures: the REDO-FIRM study. *Europace* **25**, 74–82 (2023).
14. Kaiser, B. et al. Persistent atrial fibrillation without the evidence of low-voltage areas: a prospective randomized trial. *J. Inter. Card. Electrophysiol.* **67**, 83–90 (2024).
15. Szegedi, N. et al. Long-term durability of high- and very high-power short-duration PVI by invasive remapping: The HPSD Remap Study. *Circ. Arrhythm. Electrophysiol.* **17**, e012402 (2024).
16. Mililis, P. et al. Radiofrequency versus cryoballoon catheter ablation in patients with persistent atrial fibrillation: A randomized trial. *J. Cardiovasc. Electrophysiol.* **34**, 1523–1528 (2023).
17. Wakamatsu, Y. et al. Hot balloon versus cryoballoon ablation for persistent atrial fibrillation: Lesion area, efficacy, and safety. *J. Cardiovasc. Electrophysiol.* **31**, 2310–2318 (2020).
18. Schmidt, B. et al. Laser Balloon or Wide-Area Circumferential Irrigated Radiofrequency Ablation for Persistent Atrial Fibrillation: A Multicenter Prospective Randomized Study. *Circ. Arrhythm. Electrophysiol.* **10**, e005767 (2017).
19. Reddy, V. Y. et al. Pulsed field ablation in patients with persistent atrial fibrillation. *J. Am. Coll. Cardiol.* **76**, 1068–1080 (2020).
20. Kanitsoraphan, C. et al. The efficacy of posterior wall isolation in atrial fibrillation ablation: A systematic review and meta-analysis of randomized controlled trials. *J. Arrhythm.* **38**, 275–286 (2022).
21. Gunawardene, M. A. et al. Left Atrial Posterior Wall Isolation with Pulsed Field Ablation in Persistent Atrial Fibrillation. *J. Clin. Med.* **12**, 6304, https://doi.org/10.3390/jcm12196304 (2023).
22. William, J. et al. Radiofrequency catheter ablation of persistent atrial fibrillation by pulmonary vein isolation with or without left atrial posterior wall isolation: long-term outcomes of the CAPLA trial. *Eur. Heart J*. **46**, 132–143 (2025).
23. Trayanova, N. A. & Prakosa, A. Up digital and personal: How heart digital twins can transform heart patient care. *Heart Rhythm.* **21**, 89–99 (2024).
24. Zahid, S. et al. Patient-derived models link re-entrant driver localization in atrial fibrillation to fibrosis spatial pattern. *Cardiovasc. Res.* **110**, 443–454 (2016).
25. Boyle, P. M. et al. Computationally guided personalized targeted ablation of persistent atrial fibrillation. *Nat. Biomed. Eng.* **3**, 870–879 (2019).
26. Sakata, K. et al. Assessing the arrhythmogenic propensity of fibrotic substrate using digital twins to inform a mechanisms-based atrial fibrillation ablation strategy. *Nat. Cardiovasc. Res.* **3**, 857–868 (2024).
27. Sakata, K. et al. Optimizing the distribution of ablation lesions to prevent postablation atrial tachycardia: A personalized digital-twin study. *J. Am. Coll. Cardiol. EP*. **10**, 2347–2358 (2024).
28. Yamaguchi, T. et al. Efficacy of left atrial voltage-based catheter ablation of persistent atrial fibrillation. *J. Cardiovasc. Electrophysiol.* **27**, 1055–1063 (2016).
29. Liu, E. et al. Adjunctive low-voltage burden-guided PW ablation during 1st time PVI the ALPINE randomized clinical trial. *Heart Rhythm.* **21**, S656 (2024).
30. Jadidi, A. S. et al. Ablation of persistent atrial fibrillation targeting low-voltage areas with selective activation characteristics. *Circ. Arrhythm. Electrophysiol.* **9**, e002962 (2016).
31. Nademanee, K. et al. A new approach for catheter ablation of atrial fibrillation: mapping of the electrophysiologic substrate. *J. Am. Coll. Cardiol.* **43**, 2044–2053 (2004).
32. Sakata, K. et al. The spatiotemporal electrogram dispersion ablation targeting rotors is more effective for elderly patients than non-elderly population. *J. Arrhythm.* **39**, 315–326 (2023).
33. Hayashi, K. et al. Real-time visualization of the esophagus and left atrial posterior wall by intra-left atrial echocardiography. *J. Inter. Card. Electrophysiol.* **63**, 629–637 (2022).
34. Masuda, M. et al. Long-term impact of additional ablation after pulmonary vein isolation: results from EARNEST-PVI trial. *J. Am. Heart Assoc.* **12**, e029651 (2023).
35. Della Rocca, D. G. et al. Pulsed electric field, cryoballoon, and radiofrequency for paroxysmal atrial fibrillation ablation: a propensity score-matched comparison. *Europace* **26**, euae016 (2023).
36. Haïssaguerre, M. et al. Catheter ablation of long-lasting persistent atrial fibrillation: clinical outcome and mechanisms of subsequent arrhythmias. *J. Cardiovasc. Electrophysiol.* **16**, 1138–1147 (2005).

37. Park, J. W. et al. Atrial fibrillation catheter ablation increases the left atrial pressure. *Circ. Arrhythm. Electrophysiol.* **12**, e007073 (2019).
38. Regany-Closa, M. et al. Head-to-head comparison of pulsed field ablation, very high power-short duration, cryoballoon and conventional radiofrequency ablation by LGE-MRI-based ablation lesion assessment. *Europace* **26**, euae102.212 (2024).
39. Boano, G., Vánky, F. & Åström Aneq, M. Effect of cryothermic and radiofrequency Cox-Maze IV ablation on atrial size and function assessed by 2D and 3D echocardiography, a randomized trial. To freeze or to burn. *Clin. Physiol. Funct. Imaging* **43**, 431–440 (2023).
40. Ohkura, T. et al. Comparison of maximum-sized visually guided laser balloon and cryoballoon ablation. *Heart Vessels* **38**, 691–698 (2023).
41. Huang, S. T. et al. Relationship between ablation lesion size estimated by ablation index and different ablation settings-an ex vivo porcine heart study. *J. Cardiovasc Transl. Res.* **13**, 965–969 (2020).
42. Della Rocca, D. G. et al. Targeting non-pulmonary vein triggers in persistent atrial fibrillation: results from a prospective, multicentre, observational registry. *Europace* **23**, 1939–1949 (2021).
43. Lin, W. S. et al. Catheter ablation of paroxysmal atrial fibrillation initiated by non-pulmonary vein ectopy. *Circulation* **107**, 3176–3183 (2003).
44. Rossi, V. A. et al. Predictors of left atrial fibrosis in patients with atrial fibrillation referred for catheter ablation. *Cardiol. J.* **29**, 413–422 (2022).
45. Yavin, H. et al. Atrial endocardial unipolar voltage mapping for detection of viable intramural myocardium: a proof-of-concept study. *Circ. Arrhythm. Electrophysiol.* **16**, e011321 (2023).
46. Müller, P. et al. Association of left atrial low-voltage area and thromboembolic risk in patients with atrial fibrillation. *Europace* **20**, f359–f365 (2018).
47. Chieng, D. et al. Impact of posterior left atrial voltage on ablation outcomes in persistent atrial fibrillation: CAPLA substudy. *J. Am. Coll. Cardiol. Ep.* **9**, 2291–2299 (2023).
48. Starek, Z. et al. Baseline left atrial low-voltage area predicts recurrence after pulmonary vein isolation: WAVE-MAP AF results. *Europace* **25**, euad194 (2023).
49. Caixal, G. et al. Accuracy of left atrial fibrosis detection with cardiac magnetic resonance: correlation of late gadolinium enhancement with endocardial voltage and conduction velocity. *Europace* **23**, 380–388 (2021).
50. Bansmann, P. M., Mohsen, Y., Horlitz, M. & Stöckigt, F. Optimizing fibrosis detection: a comparison of electroanatomical mapping and late enhancement gadolinium magnetic resonance imaging. *J. Inter. Card. Electrophysiol.* **67**, 571–577 (2024).
51. Lefebvre, A. L. et al. Po-05-009 combined left and right atrial network (claranet): a deep learning (dl) model for reproducible lge-mri automatic segmentation of left and right atria (la/ra) in atrial fibrillation (af) treatment planning. *Heart Rhythm.* **21**, S553–S554 (2024).
52. Pashakhanloo, F. et al. Myofiber architecture of the human atria as revealed by submillimeter diffusion tensor imaging. *Circ. Arrhythm. Electrophysiol.* **9**, e004133 (2016).
53. Roney, C. H. et al. Universal atrial coordinates applied to visualisation, registration and construction of patient specific meshes. *Med. Image Anal.* **55**, 65–75 (2019).
54. Plank, G. et al. The openCARP simulation environment for cardiac electrophysiology. *Comput. Methods Prog. Biomed.* **208**, 106223 (2021).

## Acknowledgements

We are grateful to Sanaz Norgard for her assistance with the clinical information. This study was funded by National Institutes of Health grants R01HL174440 (N.A.T.) and R01HL166759 (N.A.T., E.G.K., and D.D.S.), and a Leducq Foundation grant (N.A.T.). The funder played no role in study design, data collection, analysis and interpretation of data, or the writing of this manuscript.

## Author contributions

K.S. contributed to the study conceptualization, the DT construction and simulation, and the analysis of the simulation results and clinical data including EAM data and wrote the paper. C.A.P.Y., S.Y.A., S.L., A.P., and E.G.K. contributed to the construction and simulation of DTs and their analysis and verification. B.M.T. assisted with the software development and data management. S.K.S., J.E.M., H.C., and D.D.S. helped obtain the clinical data. N.A.T. contributed to the supervision on all aspects of the project and the preparation of the manuscript. All authors reviewed the manuscript.

## Competing interests

The authors declare no competing interests.

## Additional information

**Supplementary information** The online version contains supplementary material available at https://doi.org/10.1038/s41746-025-01625-y.

**Correspondence** and requests for materials should be addressed to Natalia A. Trayanova.